Environmental Science & Technology

pubs.acs.org/est

Article

# Ligand Effects on Biotic and Abiotic Fe(II) Oxidation by the Microaerophile *Sideroxydans lithotrophicus*

Nanqing Zhou, George W. Luther, and Clara S. Chan*

Cite This: *Environ. Sci. Technol.* 2021, 55, 9362−9371

Read Online

ACCESS | Metrics & More | Article Recommendations | Supporting Information

**ABSTRACT:** Organic ligands are widely distributed and can affect microbially driven Fe biogeochemical cycles, but effects on microbial iron oxidation have not been well quantified. Our work used a model microaerophilic Fe(II)-oxidizing bacterium *Sideroxydans lithotrophicus* ES-1 to quantify biotic Fe(II) oxidation rates in the presence of organic ligands at 0.02 atm $O_2$ and pH 6.0. We used two common Fe chelators with different binding strengths: citrate (log $K_{Fe(II)\text{-citrate}}$ = 3.20) and nitrilotriacetic acid (NTA) (log $K_{Fe(II)\text{-NTA}}$ = 8.09) and two standard humic substances, Pahokee peat humic acid (PPHA) and Suwannee River fulvic acid (SRFA). Our results provide rate constants for biotic and abiotic Fe(II) oxidation over different ligand concentrations and furthermore demonstrate that various models and natural iron-binding ligands each have distinct effects on abiotic versus biotic Fe(II) oxidation rates. We show that NTA accelerates abiotic oxidation and citrate has negligible effects, making it a better laboratory chelator. The humic substances only affect biotic Fe(II) oxidation, via a combination of chelation and electron transfer. PPHA accelerates biotic Fe(II) oxidation, while SRFA decelerates or accelerates the rate depending on concentration. The specific nature of organic-Fe microbe interactions may play key roles in environmental Fe(II) oxidation, which have cascading influences on cycling of nutrients and contaminants that associate with Fe oxide minerals.

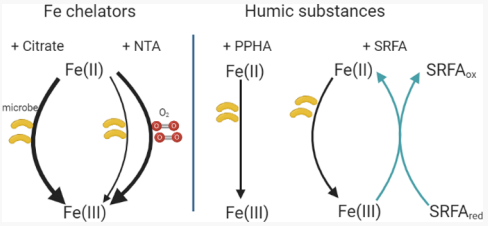


**KEYWORDS:** *Fe(II) oxidation, organic ligands, microoxic conditions, iron-oxidizing microbes*



## INTRODUCTION

Ferrous iron [Fe(II)] oxidation is a control on many biogeochemical cycles due to the association of various elements with iron oxides and oxyhydroxides.[1−5] Thus, there is a need to accurately quantify Fe(II) oxidation kinetics in natural systems, yet this remains a challenge due to the complexities of Fe(II) oxidation mechanisms. Fe(II) oxidation has largely been considered an abiotic process in which kinetics is controlled by pH,[6−8] oxidant type and concentration,[9−11] mineral surface catalysis,[12] photochemical processes,[13,14] and iron speciation, notably chelation by ligands.[7,15−18] However, microorganisms also oxidize Fe(II) in a wide range of environments, and biological Fe(II) oxidation may in fact be a dominant mechanism in oxic-anoxic transition zones where oxygen concentrations are low.[19−21] Compared to abiotic Fe(II) oxidation, there have been few systematic studies of controls on microbial Fe(II) oxidation kinetics. These have mostly explored the effects of oxidant concentration[22] and light[23] (for phototrophs), though some recent work has demonstrated that organics can alter biotic Fe(II) oxidation rates.[24−26] Given the importance of organics in terrestrial Fe cycling, organic effects on biotic Fe(II) oxidation are a major source of uncertainty in describing and predicting environmental Fe(II) oxidation.

The scope of organic effects is mostly known from previous studies on abiotic Fe(II) oxidation.[27] Under atmospheric conditions, the binding affinity of Fe chelators can affect the Fe(II) oxidation rate. Strong Fe chelators that induce high spin Fe(II) can promote abiotic Fe(II) oxidation[15,17] while weak Fe chelators might accelerate or decelerate abiotic Fe(II) oxidation depending on the pH and chelator/Fe(II) ratio.[7,13,26,28] Humic substances (HS) are also found to promote or inhibit abiotic Fe(II) oxidation given their electron-donating and electron-accepting capacities.[18,29,30] Therefore, the composition of organics combined with environmental conditions has a strong effect on abiotic Fe(II) oxidation rates. However, it is unclear if organics have the same effects on biotic Fe(II) oxidation.

Only a few studies have tested Fe(II)-oxidizing microbial activity with organic-Fe ligands. The phototroph *Rhodopseudomonas palustris* TIE-1 increased its Fe(II) oxidation rate in the presence of iron chelators citrate and EDTA and the standard HS Pahokee peat humic acid (PPHA) and Suwannee River fulvic acid (SRFA).[26] The microaerophilic chemolithotrophic Fe(II)-oxidizing bacteria (FeOB) *Sideroxydans lithotrophicus* ES-1 had higher rates of growth and biotic Fe(II) oxidation with peat-derived humic acids.[24] Similarly, a related

Received: January 26, 2021
Revised: May 28, 2021
Accepted: June 1, 2021
Published: June 10, 2021





https://doi.org/10.1021/acs.est.1c00497
*Environ. Sci. Technol.* 2021, 55, 9362−9371

FeOB, *Sideroxydans sp.* CL21, showed a 50% increase in Fe(II) oxidation rates in the presence of peat extracts.[31] In all, the work to date suggests that organics have a substantial effect on microbial iron oxidation. However, given that organics can also have an effect on abiotic Fe(II) oxidation, we must be careful to account for abiotic kinetics when we measure biotic effects. Kopf et al.[32] observed that ligands can accelerate abiotic Fe(II) oxidation by nitrite in nitrate-reducing Fe(II)-oxidizing cultures and therefore can increase abiotic competition with biotic Fe(II) oxidation. Abiotic oxidation can also be driven by $O_2$, but at micromolar $O_2$ concentrations, lithoautotrophic Fe(II)-oxidizers like *Sideroxydans* dominate Fe(II) oxidation.[20,33] Yet it is still unknown how organics might affect the balance of biotic and abiotic Fe(II) oxidation kinetics in microaerobic conditions that are typical of oxic-anoxic interfaces.

To address this, we conducted kinetics experiments with *Sideroxydans lithotrophicus* ES-1, a facultative microaerophilic FeOB that was isolated from groundwater.[34] ES-1 is unusual among microaerophilic FeOB isolates in that it can also grow on thiosulfate. This is important for kinetics measurements because we can use thiosulfate-grown ES-1 in our experiments to avoid adding Fe(III) oxyhydroxides and therefore minimize autocatalysis of Fe(II) on the mineral surfaces. Using thiosulfate-grown ES-1 cells, we investigated the effect of different types of organics on biotic and abiotic Fe(II) oxidation. We chose two Fe chelators with different binding affinities: citrate (CIT) (log $K_{Fe(II)\text{-citrate}}$ = 3.20)[35] and nitrilotriacetic acid (NTA) (log $K_{Fe(II)\text{-NTA}}$ = 8.09).[35] These are commonly used in laboratory culturing of Fe-metabolizing bacteria to avoid Fe(III)-mineral formation.[36,37] We also chose two standard HS, PPHA and SRFA, to represent natural organic matter from terrestrial and aquatic environments. The kinetics of Fe(II) oxidation with each of these four ligands were quantified at a range of different concentrations to elucidate their roles in promoting or inhibiting microbial Fe(II) oxidation under relevant laboratory and environmental conditions.

## MATERIALS AND METHODS

**Bacterial Strain and Cultivation.** *Sideroxydans lithotrophicus* ES-1 was routinely cultivated in Modified Wolfe's Minimal Medium (MWMM) buffered with 20 mM 2-(*N*-morpholino)ethanesulfonic acid (MES) at pH 6.0. To avoid Fe(III) oxide formation, 10 mM thiosulfate was used as the electron donor. Both Wolfe's vitamins and trace minerals[38] were supplemented in a 1:1000 ratio into the media after autoclaving. The headspace was maintained at 2% $O_2$, 20% $CO_2$, and 78% $N_2$ by refreshing the headspace daily.

**Experimental Setup.** The Fe(II) oxidation kinetics experiments were performed in open mouth 10 mL vials. A constant gas mix ($O_2/CO_2/N_2$ = 2:20:78) was bubbled into the vials to keep the oxygen concentration constant. Thiosulfate-grown ES-1 culture in the late-log phase (1 mL) was diluted with 4 mL of 50 mM MES buffered-MWMM (pH 6.0) to create a 5 mL reaction system. The cell density was $2.0 \times 10^7$ cells per mL in the CIT/NTA experiments and $1.5 \times 10^7$ cells per mL in the PPHA/SRFA experiments. The cell numbers were constant during the experimental time period given the long doubling time of ES-1 (8−12 h). To exclude the effects of metabolic products and thiosulfate, the same volume (1 mL) of filter-sterilized original ES-1 culture was added to 4 mL of 50 mM MES buffered-MWMM (pH 6.0) as the abiotic control. Ferrous chloride ($FeCl_2$) was used as the Fe(II) source, and the initial concentration added was 100 $\mu$M. Chelators including CIT as sodium citrate and NTA were added to final concentrations of 0, 50, 100, 200, 500, and 1000 $\mu$M, respectively, to achieve the chelator/Fe(II) ratios of 0, 0.5, 1, 2, 5, and 10. Standard HS (PPHA: 1S103H and SRFA: 2S101F) were purchased from the International Humic Substances Society (IHSS). The commercial HS were dissolved in MWMM buffered with 50 mM MES (pH 6.0) to prepare a 500 mg/L stock solution. The stock solution was stirred overnight and then filter-sterilized through a 0.22 $\mu$m nylon filter membrane. The stock solutions were diluted into 50 mM MES buffered-MWMM culture to prepare a series of concentrations of PPHA and SRFA (0, 1, 5, 25, 50, and 100 mg/L). Samples were taken at different time points, and the Fe(II) concentration was determined using the phenanthroline assay.[39] The dissolved oxygen (DO) concentration was measured before and after the kinetics experiment using a Firesting Optical Oxygen Meter (PyroScience). The DO concentration was maintained constant at ∼30 $\mu$M. All Fe(II) oxidation experiments were performed in duplicate.

**Computation and Calculation.** The distribution of Fe(II) species was calculated computationally using the Visual MINTEQ equilibrium speciation model (v3.1).[40] The speciation in cultures with HS was run using the NICA−Donnan model,[41] since the NICA−Donnan model has been reported to show a stronger correlation with experimental spectral data.[42,43]

**Fe(II) Oxidation Kinetics Analysis.** *Total Fe(II) Oxidation.* The total Fe(II) oxidation kinetics are the sum of biotic and abiotic Fe(II) oxidation kinetics

$$-\frac{d[\mathrm{Fe(II)}]\mathrm{total}}{dt} = -\left(\frac{d[\mathrm{Fe(II)}\mathrm{abio}]}{dt} + \frac{d[\mathrm{Fe(II)}\mathrm{bio}]}{dt}\right) \quad (1)$$

The phenanthroline assay measured $[Fe(II)_{total}]$ and $[Fe(II)_{abio}]$ at different time points. Therefore, total Fe(II) loss ($[Fe(II)_{total\ loss}]_t$) can be calculated by $[Fe(II)_{total}]_-[Fe(II)_{total}]_t$, and abiotic Fe(II) loss ($[Fe(II)_{abio\ loss}]_t$) can be calculated by $[Fe(II)_{abio}]_0-[Fe(II)_{abio}]_t$. Therefore, the biotic Fe(II) loss ($[Fe(II)_{bio\ loss}]_t$) is $[Fe(II)_{total\ loss}]_t-[Fe(II)_{abio\ loss}]_t$. The biological contribution on Fe(II) oxidation is calculated by

$$\text{biological contribution } (\%)_t = 100 \times \frac{[\mathrm{Fe(II)}_{\text{total loss}}]_t - [\mathrm{Fe(II)}_{\text{abio loss}}]_t}{[\mathrm{Fe(II)}_{\text{total loss}}]_t} \quad (2)$$

*Abiotic Fe(II) Oxidation.* Since ES-1 cells grown on thiosulfate were used as the inoculum, the heterogeneous Fe(II) oxidation is negligible, only homogeneous aqueous Fe(II) oxidation by DO was considered.

When the organic ligands are absent, the Fe(II) oxidation reaction is as follows:

$$\mathrm{Fe(II)_{aq}} + 0.25O_2 + 2.5H_2O \rightarrow \mathrm{Fe(OH)_3} + 2H^+ \quad (3)$$

We acknowledge that there are varied Fe(III) products in our system (e.g., $Fe(OH)_2^+$), which would alter $[H^+]$ in eq 3 and the subsequent eq 4; however, pH is kept constant in our experiments.

Applying the rate law to eq 3, the abiotic Fe(II) oxidation rate can be described as eq 4:[44]



https://doi.org/10.1021/acs.est.1c00497
Environ. Sci. Technol. 2021, 55, 9362−9371

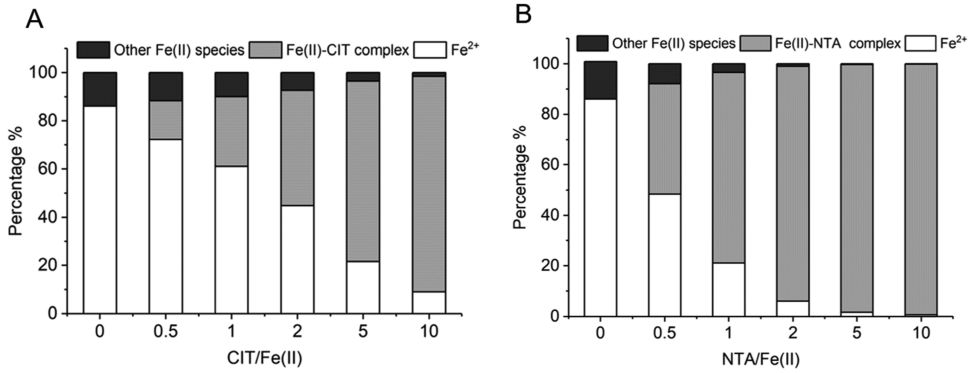


**Figure 1.** Fe(II) species distribution of different chelators/Fe(II) molar ratios in (A) CIT and (B) NTA cultures. The Fe(II)−CIT complex includes Fe-CIT and FeH-CIT. The Fe(II)−NTA complex includes Fe-NTA and FeH-NTA. Other Fe(II) species include $FeOH^+$, $FeCl^+$, $FeSO_4$, $FeNH_3^{2+}$, $FeH_2PO_4^+$, $FeHPO_4$, and $FeHCO_3^+$, but there is no $FeOH^+$ when NTA/Fe(II) ≥ 1 (Table S1A and S3A).

$$-\frac{d[\mathrm{Fe(II)}_{aq}]}{dt} = k_{\mathrm{Fe(II)}_{abio}}[\mathrm{Fe(II)}_{aq}][O_2]/[H^+]^2 \quad (4)$$

When there are organic ligands present, the reaction can be described as follows:[15]

$$\mathrm{Fe(II)} - L + O_2 + \rightarrow Fe(III) - L + O_2^{\bullet -} \quad (5)$$

$$-\frac{d[\mathrm{Fe(II)} - L]}{dt} = k_{\mathrm{Fe(II)-L}_{abio}}[Fe(II) - L][O_2] \quad (6)$$

Since the dissolved $O_2$ concentration and pH remain constant during the experiment, the rate constant could be simplified as $k'_{\mathrm{Fe(II)abio}} = k_{\mathrm{Fe(II)abio}}[O_2]/[H^+]^2$, $k'_{\mathrm{Fe(II)-Labio}} = k_{\mathrm{Fe(II)-Labio}}[O_2]$. Thus, the reactions should fit pseudo-first-order kinetics.

Therefore, the rate law of the abiotic Fe(II) oxidation can be described as eq 7:[7,45]

$$-\frac{d[\mathrm{Fe(II)}_{abio}]}{dt} = k'_{\mathrm{Fe(II)}_{abio}}[\mathrm{Fe(II)}_{aq}] + k'_{\mathrm{Fe(II)-L}_{abio}}[\mathrm{Fe(II)} - L] \quad (7)$$

*Biotic Fe(II) Oxidation.* The enzymatic Fe oxidation is catalyzed by the cytochromes in the cell outer membrane. Therefore, the reaction can be described as

$$\mathrm{Fe(II)}_{aq} + \mathrm{cyt}_{ox} + 3H_2O \rightarrow \mathrm{Fe(OH)}_3 + \mathrm{cyt}_{red} + 3H^+ \quad (8)$$

$$\mathrm{Fe(II)} - L + \mathrm{cyt}_{ox} \rightarrow \mathrm{Fe(III)} - L + \mathrm{cyt}_{red} \quad (9)$$

Since the microbially catalyzed Fe(II) oxidation has been reported to fit either zeroth or pseudo-first-order rate law,[20,46] the kinetics can be described as

$$-\frac{d[\mathrm{Fe(II)}_{bio}]}{dt} = k_{bio} \quad (10)$$

or

$$-\frac{d[\mathrm{Fe(II)}_{bio}]}{dt} = k_{bio}[\mathrm{Fe(II)}_{bio}] \quad (11)$$

$k_{bio}$ then can be derived from linear or exponential fitting from $[Fe(II)_{bio}]_t$ and time. If the R-squared value for a zero-order reaction is equal to or higher than that for the first-order reaction, then a zero-order reaction should be the better model.[46] In our experiment, the units of the zero-order rate constant are $\mu M\ min^{-1}$, whereas the units of the first-order reaction rate constant are $min^{-1}$.

The microbial Fe(II) oxidation rates ($\mu$mol cell$^{-1}$ h$^{-1}$) were calculated by[20]

$$\text{microbial Fe(II) ox. per cell} = [\mathrm{Fe(II)}_{bio}]_t \times t^{-1} \times (\text{cell num})^{-1} \quad (12)$$

For the zeroth order reaction, the microbial Fe(II) oxidation rates ($\mu$mol cell$^{-1}$ h$^{-1}$) could be simplified as

$$\text{microbial Fe(II) ox. per cell} = k_{bio} \times (\text{cell num})^{-1} \quad (13)$$

## RESULTS AND DISCUSSION

**The Effect of Fe Chelators.** CIT and NTA are both polycarboxylates, but the nitrogen in the NTA structure can react with the metal ion, which makes the complex more stable than the metal−CIT complex.[47] The Visual MINTEQ calculation of Fe(II) species showed that as the concentration of chelators increases, the proportion of each Fe(II)−chelator complex also increases (Figure 1; details of Fe(II) species distribution in Tables S1A, 1B and S3A, 3B). Moreover, the proportion of Fe(II) as Fe(II)-NTA was higher than Fe(II)-CIT given the same chelator/Fe(II) ratio (Figure 1) because other cations such as $Ca^{2+}$ and $Mg^{2+}$ compete with $Fe^{2+}$ for CIT but not NTA complexation in the media. The stability constants of Ca(II)-CIT (log $K$ = 3.50)[48] and Mg(II)-CIT (log $K$ = 3.73)[49] are higher than that of Fe(II)-CIT (log $K$ = 3.20)[35] and the concentration of the two cations is also higher than that of $Fe^{2+}$ in the media ($Ca^{2+}$ = 900 $\mu$M, $Mg^{2+}$ = 813 $\mu$M). Therefore, a large proportion of CIT is complexed with $Ca^{2+}$ and $Mg^{2+}$ instead of $Fe^{2+}$ (Table S1B). The stability constant of Fe(II)-NTA (log $K$ = 8.09)[35] is several orders of magnitude higher than that of Ca(II)-NTA (log $K$ = 6.40)[35] and Mg(II)-NTA (log $K$ = 5.50).[35] In this case, $Ca^{2+}$ and $Mg^{2+}$ cannot outcompete $Fe^{2+}$ for NTA complexation.

The Fe(II) oxidation kinetics in the presence of CIT show that biotic Fe(II) oxidation was predominant (Figure S1A) and abiotic oxidation was negligible (Figure S1B) in our experiments in which the oxygen saturation was 14% (~30 $\mu$M). The analysis of Fe(II) oxidation time-course curves shows that the data fit a zeroth order rate law, since the R-squared values are larger in zeroth order fitting than in the pseudo-first-order fitting (Table S2), which is consistent with microbially catalyzed Fe(II) oxidation kinetics.[46] The rate


https://doi.org/10.1021/acs.est.1c00497
Environ. Sci. Technol. 2021, 55, 9362−9371

constants calculated from the zeroth order rate law showed that the biotic rate constant does not vary, aside from CIT/Fe(II) = 2, which could be an outlier (Figure 2 and Table 1).

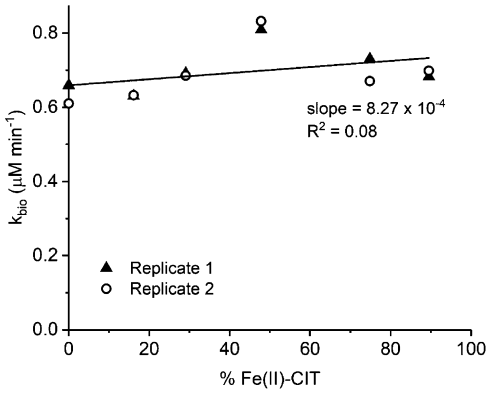


**Figure 2.** Biotic zeroth order rate constants ($k_{bio}$) at different Fe(II)-CIT proportions show that the rate constants are stable with the Fe(II)-CIT proportion increase (except for one outlier). The $R^2$ value is the adjusted $R^2$.

Our results suggest that CIT does not affect biotic or abiotic Fe(II) oxidation under these microoxic conditions because the labile Fe(II)−CIT complex dissociates quickly to free Fe(II), so that the cells are using free Fe(II) even though CIT is present.

Unlike CIT, NTA is an inert chelator of Fe(II); that is, Fe(II)-NTA cannot as easily dissociate to provide free Fe(II). The addition of NTA increased the total Fe(II) oxidation rate in ES-1 culture with the increasing NTA/Fe(II) molar ratio, and the enhancement was mainly due to the promotion of abiotic Fe(II) oxidation (Figure S2). The abiotic Fe(II) oxidation fits a pseudo-first-order rate law, and the rate constant $k_{abio}$ was linearly related to the % of Fe(II) as Fe(II)-NTA (Table S4A). The amount of Fe(II) oxidized by microbes at each time point was calculated from the data in Figure S2 according to eq 1. When the ratio of NTA/Fe(II) is zero and there are no cells, the reaction of this low amount of $O_2$ with free Fe(II) is negligible (Figure S2B). The difference between initial Fe(II) (at time 0) and the measured Fe(II) at any point in Figure S2B gives the amount of abiotic Fe(II) loss due to abiotic oxidation. The difference between initial Fe(II) and the measured Fe(II) at any point in Figure S2A gives the total amount of Fe(II) loss to abiotic and biotic oxidation. The difference between the Fe(II) loss in Figure S2A and Figure S2B at each time point gives the Fe(II) loss to biotic oxidation.

The biotic Fe(II) oxidation fits the zeroth order rate law (Table S4B), and the rate constant ($k_{bio}$) decreased with the % Fe(II)−NTA complex. Both $k_{abio}$ and $k_{bio}$ are linearly correlated with the % of Fe(II)-NTA but in opposite directions (Figure 3A). The biological contribution to Fe(II) oxidation was calculated by averaging the $(Fe(II)_{total\ loss} - Fe(II)_{abiotic\ loss})/Fe(II)_{total\ loss}$, and it also fits a linear model ($R^2$ = 0.97) with the % Fe(II)−NTA complex in the culture (Figure 3B). NTA is able to push electron density in both $\sigma$ and $\pi$ bonding to Fe(II), which allows Fe(II) to reduce $O_2$ more efficiently than free Fe(II).[50] Therefore, Fe(II)-NTA has a higher abiotic reaction rate with $O_2$ (Table 2). The increase of NTA/Fe(II) resulted in a higher % Fe(II)−NTA complex, which corresponded to higher abiotic Fe(II) oxidation rates and lowered the relative biological contribution to Fe(II) oxidation (Figure 3B).

In FeOB laboratory culturing, CIT and NTA can both be used as chelators to prevent Fe oxyhydroxide formation,[36,37] but CIT is a better choice because it has no effect on either biotic or abiotic Fe(II) oxidation. If NTA is chosen, more Fe(II) needs to be supplied in FeOB culturing to compensate for abiotic oxidation.

**The Effect of Humic Substances.** HS represent natural organic matter in that they have a range of different functional groups, which can cause them to not only chelate Fe(II) but also be redox active.[51−53] Systematic electrochemical studies have quantified the electron-donating capacities (EDC) and electron-accepting capacities (EAC) of HS.[54−56] Differences in HS chemistry and concentration have the potential to cause varied effects on Fe(II) during oxidation. Visual MINTEQ calculations show that with higher concentrations of PPHA and SRFA, more Fe(II) is complexed by each HS (Figure 4). Compared to PPHA, more Fe(II) was complexed with SRFA given the same HS concentration. Our calculations show that more than 50% of Fe(II) combines with SRFA when the SRFA concentration is 100 mg/L, whereas only 33% of Fe(II) complexes with PPHA at the same concentration (Table S5 and S7). The higher % complexation with SRFA is because SRFA has a higher number of carboxylate functional groups in its structure.[57−59]

The Fe(II) oxidation kinetics results showed similar results to citrate (Figure S1) in that the oxidation kinetics with PPHA fit a zeroth order rate law, consistent with microbially catalyzed oxidation (Table 3, Figure S3, Table S6). When the PPHA concentration was 0−5 mg/L, there was negligible effect on the Fe(II) oxidation rate (Figure S3, Table 3). The Visual MINTEQ calculation showed that less than 2% of Fe(II) was complexed at PPHA concentrations of 0−5 mg/L (Table 3). When the PPHA concentration was 25 mg/L or higher, Fe(II) oxidation was promoted (Figure S3, Table 3). Moreover, when the PPHA concentration was high (≥50 mg/L), PPHA had little effect on the abiotic Fe(II) oxidation at the initial stage (up to 45 min), which means that PPHA mainly promoted biotic Fe(II) oxidation during the beginning of Fe(II)

**Table 1. Parameters of Fe(II)-CIT Oxidation**[a]

| CIT/Fe | Fe(II)-CIT(%) | $k_{total}$ (μM min$^{-1}$) | $k_{abio}$ (μM min$^{-1}$) | $k_{bio}$ (μM min$^{-1}$) | biotic Fe oxidation (%) | biotic Fe oxidation rate (μmol/cell/h) |
|---|---|---|---|---|---|---|
| 0 | 0.00 | 0.6351 | 0 | 0.6351 | 100 | 1.91E-09 |
| 0.5 | 16.12 | 0.6318 | 0 | 0.6318 | 100 | 1.90E-09 |
| 1 | 29.07 | 0.6885 | 0 | 0.6885 | 100 | 2.06E-09 |
| 2 | 47.83 | 0.8208 | 0 | 0.8208 | 100 | 2.46E-09 |
| 5 | 74.85 | 0.7005 | 0 | 0.7005 | 100 | 2.10E-09 |
| 10 | 89.52 | 0.6905 | 0 | 0.6905 | 100 | 2.07E-09 |

[a]Note: the $k_{total}$ and $k_{bio}$ were calculated from the average of duplicates.



https://doi.org/10.1021/acs.est.1c00497
Environ. Sci. Technol. 2021, 55, 9362−9371

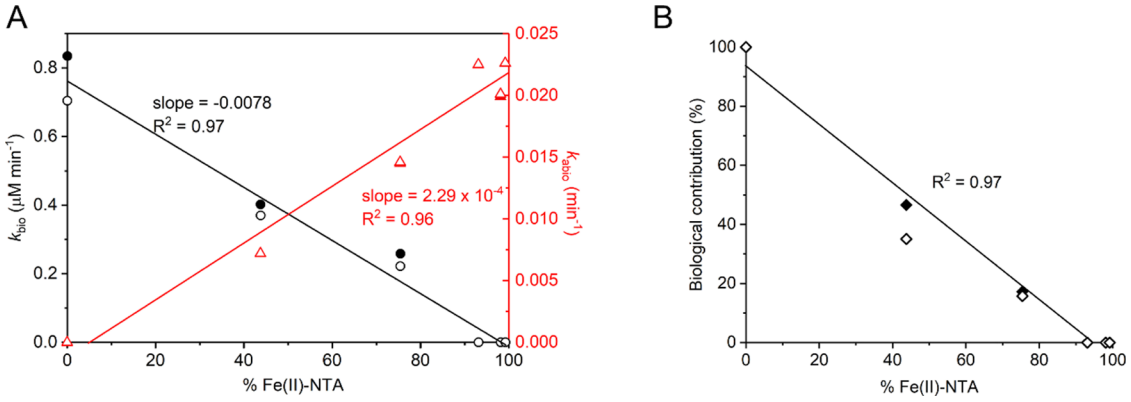


**Figure 3.** Linear fitting of (A) biotic and abiotic rate constant with Fe(II)-NTA proportion and (B) biological contribution to Fe(II) oxidation with Fe(II)-NTA percentage. The open and closed symbols (circle, triangle, and diamond) represent the two replicates.

**Table 2. Parameters of Fe(II)-NTA Oxidation**[a]

| NTA/Fe(II) | Fe(II)-NTA(%) | $k_{abio}$ ($min^{-1}$) | $k_{bio}$ ($\mu M\ min^{-1}$) | biotic Fe oxidation (%) | biotic Fe oxidation rate ($\mu$mol/cell/h) |
|---|---|---|---|---|---|
| 0 | 0 | 0 | 0.7694 | 100 | 2.31E-09 |
| 0.5 | 43.75 | 0.0072 | 0.3860 | 41.82 | 1.16E-09 |
| 1 | 75.40 | 0.0146 | 0.2401 | 16.41 | 7.20E-10 |
| 2 | 93.10 | 0.0225 | 0 | 0 | 0 |
| 5 | 98.14 | 0.0200 | 0 | 0 | 0 |
| 10 | 99.20 | 0.0226 | 0 | 0 | 0 |

[a]Note: the $k_{total}$ and $k_{bio}$ were calculated from the average of duplicates.

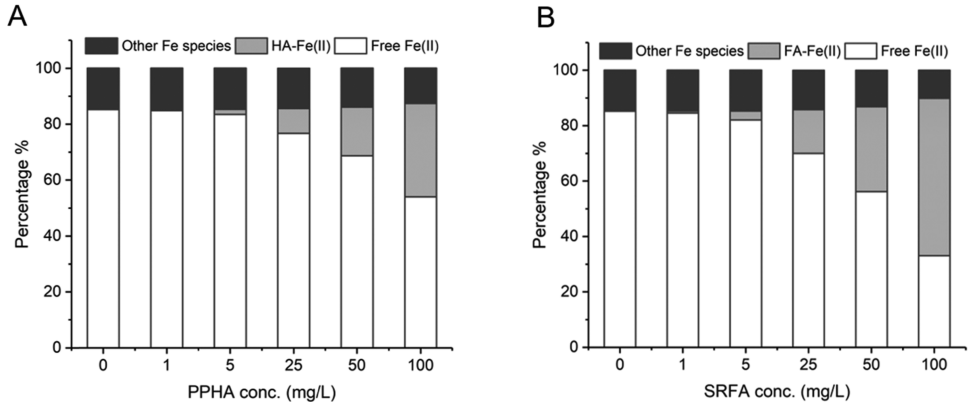


**Figure 4.** Fe(II) species distribution in (A) PPHA and (B) SRFA cultures, as calculated by Visual MINTEQ. HA-Fe(II) includes HA1-Fe(II) and HA2-Fe(II), while FA-Fe(II) only contains FA1-Fe(II). Other Fe(II) species include $FeOH^+$, $FeCl^+$, $FeSO_4$, $FeNH_3^{2+}$, $FeH_2PO_4^+$, $FeHPO_4$, $FeHCO_3^+$, and (6)$Fe^{2+}$D(aq), which represents weakly electrostatically bound Fe to dissolved humic acids (Table S5 and S7).

**Table 3. Parameters of Fe(II)-PPHA Oxidation**[a]

| PPHA conc. (mg/L) | C/Fe | Fe(II)-PPHA(%) | $k_{total}$ ($\mu M\ min^{-1}$) | $k_{abio}$ ($min^{-1}$) | $k_{bio}$ ($\mu M\ min^{-1}$) | biotic Fe oxidation (%) | biotic Fe oxidation rate ($\mu$mol/cell/h) |
|---|---|---|---|---|---|---|---|
| 0 | 0 | 0.00 | 0.3918 | 0 | 0.3918 | 100 | 1.57E-09 |
| 1 | 0.1 | 0.36 | 0.4020 | 0 | 0.4020 | 100 | 1.61E-09 |
| 5 | 0.5 | 1.80 | 0.4084 | 0 | 0.4084 | 100 | 1.63E-09 |
| 25 | 2.5 | 8.89 | 0.4534 | 0 | 0.4534 | 100 | 1.81E-09 |
| 50 | 5 | 17.44 | 0.5784 | 0 | 0.5784 | 100 | 2.31E-09 |
| 100 | 10 | 33.44 | 0.7220 | 0 | 0.7220 | 100 | 2.89E-09 |

[a]Note: the $k_{total}$ and $k_{bio}$ were calculated from the average of duplicates.

oxidation. After the first 45 min, abiotic Fe(II) oxidation (only 20% based on total Fe(II)) began in the filter-sterilized control. However, this delayed abiotic oxidation is not apparent in the live culture experiment since the Fe(II) concentration change is smooth (Figure S3). Thus, for 50 and 100 mg/L of PPHA, we calculated $k_{bio}$ using the data up until 45 min. The $k_{bio}$ values fit a linear model with the PPHA concentration increase (Figure 5).

PPHA covers a wide range of reduction potentials ($E_h$) (0 to −490 mV) with the apparent $E_h$ of −122 mV at pH 7[56] and



https://doi.org/10.1021/acs.est.1c00497
Environ. Sci. Technol. 2021, 55, 9362−9371

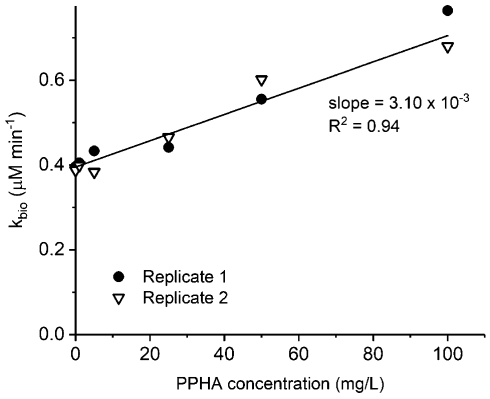


**Figure 5.** Linear fitting of biotic Fe(II) oxidation rate constants ($k_{bio}$) with PPHA concentration shows that $k_{bio}$ increases with increasing PPHA concentration. The $k_{bio}$ up to 45 min was used when the PPHA concentration was 50 and 100 mg/L PPHA.

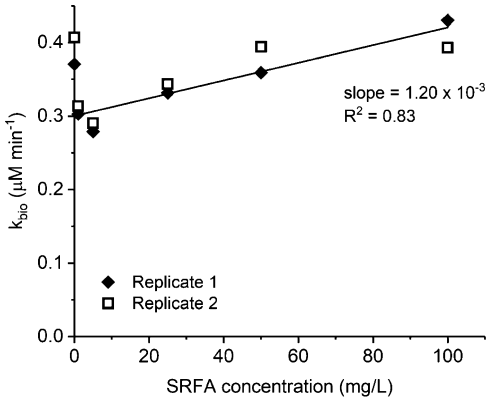


**Figure 6.** Change of the biotic Fe(II) oxidation rate constant ($k_{bio}$) in the presence of different concentrations of SRFA. $k_{bio}$ decreases with the increasing SRFA concentration when SRFA < 5 mg/L and increases with SRFA concentration when SRFA ≥ 5 mg/L. This increasing portion fits a linear model.

the calculated $E_h$' at pH 6 is −63 mV. The EAC and EDC were measured to be 1.7 and 2.2 mmol $e^-$/g HS using an electrode poised at −0.49 and + 0.73 V (pH 7), respectively.[58] Therefore, the promotion of biotic Fe(II) oxidation is likely due to PPHA having both high EAC and EDC to act as an electron shuttle to facilitate electron transfer between Fe(II) and cells, since microaerophilic FeOB oxidize Fe(II) extracellularly. It is unknown what caused the delayed abiotic Fe(II) oxidation in the filter-sterilized control at high PPHA concentrations (50 and 100 mg/L). One explanation may be the slow formation of nanometer-scale Fe(III) oxyhydroxides and the resulting mineral-catalyzed heterogeneous oxidation.[60−62] Slow Fe(II) oxidation in the presence of HS favors the formation of ferrihydrite over organic-bound Fe(III),[63] and at the same time, the presence of high PPHA concentrations coating the ferrihydrite prevents its aggregation into larger particles, resulting in a high surface area for autocatalyzed Fe oxidation.[64−66]

SRFA influenced biotic Fe(II) oxidation but had no effect on abiotic Fe(II) oxidation (Table 4, Figure S4), and the biotic oxidation kinetics fit a zeroth order rate law (Table S8). The biotic Fe(II) oxidation rate (and total rate) decreased with the first addition of SRFA (1 mg/L) and then increased as the SRFA concentration increased (Table 4, Figure 6). In addition, $k_{bio}$ fits a linear model with the SRFA concentration increase (Figure 6). Since the rate constant for SRFA at 0 mg/L agreed within 1% of that for 0 mg/L PPHA ($k_{bio}$ = 0.3903 ± 0.0153, $n$ = 4), we consider the cell behavior in these two experiments as similar. Therefore, the slope of $k_{bio}$-HS can be used to compare the impact of different HS. The slope of $k_{bio}$-HS for SRFA is 39% of that of PPHA (from Figures 5 and 6), showing that different HS have different effects on biotic Fe(II) oxidation. Overall, the results suggest that there are competing effects on biotic Fe(II) oxidation in the presence of SRFA.

The competing effects can be explained by the redox balance between the Fe(III)-reducing groups and the Fe(III)-binding groups in SRFA. SRFA, with a calculated $E_h$' of +182 mV at pH 6 based on the measured value,[67] showed slightly higher EDC (2.8 mmol $e^-$/g HS) but much lower EAC (0.67 mmol $e^-$) than PPHA measured at the same poised electrode potentials at pH 7,[58] which makes SRFA a better electron donor. Pullin and Cabaniss[6,68] and Garg et al.[69] demonstrated that thermal reduction of Fe(III) by SRFA occurs in dark conditions at pH 6.0−8.7. Our work also showed a decreased net biotic Fe(II) oxidation rate with the addition of low concentrations of SRFA, which is due to the Fe(III) thermal reduction. However, when the SRFA concentration increased, a higher proportion of Fe(III)-SRFA formed. Voelker et al.[70] showed that Fe(III)-SRFA is a less reducible Fe(III) form, which increased the net Fe(II) oxidation rate at a higher SRFA concentration. The competing effect has also been observed in Cu(II) reduction. Pham et al.[71] showed that the high concentration of SRFA can form a nonreducible stable complex with Cu(II) and prevent Cu(II) from reduction by SRFA.

In summary, the HS used in this study affect only biotic Fe(II) oxidation at 30 μM $O_2$, and the HS composition determines their impact on the oxidation rate. The terrestrial HS PPHA acts as an electron shuttle to accelerate electron transfer between Fe(II) and FeOB. The aquatic HS SRFA can reduce some of the produced Fe(III), which reduces net Fe(II) oxidation rates at most of the SRFA concentrations tested. Nevertheless, oxidation rates increase at higher SRFA. Given the contrasting effects of PPHA and SRFA, the molecular

**Table 4. Parameters of Fe(II)-SRFA Oxidation**[a]

| SRFA conc. (mg/L) | C/Fe | Fe(II)-SRFA (%) | $k_{total}$ (μM $min^{-1}$) | $k_{abio}$ ($min^{-1}$) | $k_{bio}$ (μM $min^{-1}$) | biotic Fe oxidation (%) | biotic Fe oxidation rate (μmol/cell/h) |
|---|---|---|---|---|---|---|---|
| 0 | 0 | 0 | 0.3888 | 0 | 0.3888 | 100 | 1.56E-09 |
| 1 | 0.09 | 0.63 | 0.3084 | 0 | 0.3084 | 100 | 1.23E-09 |
| 5 | 0.47 | 3.14 | 0.2847 | 0 | 0.2847 | 100 | 1.14E-09 |
| 25 | 2.32 | 15.36 | 0.3376 | 0 | 0.3376 | 100 | 1.35E-09 |
| 50 | 4.65 | 29.82 | 0.3767 | 0 | 0.3767 | 100 | 1.51E-09 |
| 100 | 9.35 | 55.32 | 0.4116 | 0 | 0.4116 | 100 | 1.65E-09 |

[a]Note: the $k_{total}$ and $k_{bio}$ were calculated from the average of duplicates.



https://doi.org/10.1021/acs.est.1c00497
Environ. Sci. Technol. 2021, 55, 9362−9371

composition of HS is a key factor when evaluating their effects on Fe(II) oxidation.

## ■ ENVIRONMENTAL IMPLICATIONS

To understand the interactions between organics and Fe(II) oxidation in the environment, we need to consider the range of realistic conditions and mechanisms to determine the primary controls on oxidation rates. A challenge is that the environment includes many permutations of pH, temperature, organic, and solute compositions. Previous studies show that these variables can have interrelated and competing effects on Fe(II) oxidation kinetics (Table S9 and references therein). However, a key variable in Fe(II) oxidation kinetics is oxygen concentration, but the effects of oxygen are rarely explored, as almost all abiotic studies of organic-Fe(II) oxidation focus on fully oxygenated conditions. Yet, in the environment, Fe(II) more commonly exists in suboxic environments, and chemical Fe(II) oxidation rates are orders of magnitude slower at low $O_2$ concentrations.[44] Chen et al.[72] and Liang et al.[9] found that this is also true in the presence of natural organic matter (NOM), including SRFA, freshwater-derived NOM, and polyglutamate. Our work also showed that abiotic Fe(II) oxidation was slow or negligible in the presence of natural occurred organics (citrate, SRFA, and PPHA). In total, work to date suggests slow abiotic oxidation at low $O_2$ concentrations in the presence of organics, which would allow microbial Fe(II) oxidation to be a prominent mechanism.

Indeed, we found that a microaerophilic FeOB catalyzed the bulk of Fe(II) oxidation in the presence of NOM. With our work, there are now several studies on both anaerobic and microaerophilic Fe(II) oxidizers, which generally show the dominance of microbial Fe(II) oxidation over abiotic Fe(II) oxidation. While the biotic oxidation rates in our study are within the range of other reported rates, specific effects of organics differ between the studies, which use different FeOB (Table S10). One explanation may be the different pH optima of these FeOB, since pH can change the redox potentials and complexation behavior of organic ligands. Increasing pH is associated with a decrease of the Fe(III) reduction rate by SRFA,[6] and this may partly account for the different results for *Sideroxydans* (pH 6) and photoautotrophic FeOB (pH 7).[26,73] Another explanation may be that FeOB have various Fe(II)-oxidizing mechanisms that interact differently with organic-Fe(II). Nitrate-reducing FeOB like *Acidovorax* indirectly oxidize Fe(II) via nitrite formed in the periplasm,[74,75] so oxidation rates may be reduced if the organic complexed Fe(II) cannot pass through cell membranes, which may account for inhibition of Fe(II) oxidation in nitrate-reducing FeOB[76] (Table S10). FeOB like *Sideroxydans* oxidize Fe(II) using outer membrane cytochromes, which evidently can interact faster with organic-Fe(II). This has implications in Fe- and organic-rich environments, as shown in a series of studies of the Schlöppnerbrunnen fen by Küsel and others.[24,25,77,78] These studies showed that *Sideroxydans* were present in the Fe-rich fen, associated with Fe(II) oxidation, and further that fen-derived peat extracts accelerated Fe(II) oxidation and growth of *Sideroxydans* strains. We showed that PPHA promoted biotic Fe(II) oxidation, in agreement with the fen *Sideroxydans* studies.[24,25] All together, these initial studies point toward the importance of microbe-organic-Fe interactions in modulating environmental Fe(II) oxidation though organics may have differing effects on different microorganisms.

Our work showed the contrasting effects of various representative organic ligands on Fe(II) oxidation by a specific microorganism, quantifying both abiotic and biotic effects on kinetics. Strong Fe chelators like NTA with a higher binding affinity accelerate abiotic Fe(II) oxidation, which reduces the biological contribution to total Fe(II) oxidation, whereas weak Fe chelators that form a labile Fe−ligand complex (e.g., citrate) have no effect on the biotic or abiotic Fe(II) oxidation rate. HS of different origins showed different effects on biotic Fe(II) oxidation due to chelation and variations in their electron-donating and electron-accepting capacity. Since NOM is a combination of different molecules,[79,80] our results indicate the net effect of NOM on Fe(II) oxidation will depend on the overall composition.

This work highlights an emerging dimension of organic carbon−iron interactions, showing how they can act as a throttle on microbially catalyzed Fe(II) oxidation. Because this is also true of microbial Fe(III) reduction,[81−83] organic ligands can strongly control the rate and balance of microbially driven Fe redox cycling. The balance depends on competing effects, so further work is needed to explore mixtures of different ligands, FeOB, and Fe(II)-reducing microbes. Although the numerous mechanisms of environmental iron transformations may seem too complex to deconstruct, this work shows that it is in fact possible to systematically quantify the interplay of microbial and abiotic mechanisms that underpin natural cryptic iron cycles, which drive transformation of key environmental nutrients and contaminants.

## ■ ASSOCIATED CONTENT

### Supporting Information

The Supporting Information is available free of charge at https://pubs.acs.org/doi/10.1021/acs.est.1c00497.

Additional information on the phenanthroline assay, kinetics data (Fe(II) concentrations over time), Visual-MINTEQ and rate law fitting calculations, and comparisons with previous literature data (PDF)

## ■ AUTHOR INFORMATION


### Corresponding Author

**Clara S. Chan** − *School of Marine Science and Policy and Department of Earth Sciences, University of Delaware, Newark, Delaware 19716, United States;* orcid.org/0000-0003-1810-4994; Phone: (302) 831-1819; Email: cschan@udel.edu

### Authors

**Nanqing Zhou** − *School of Marine Science and Policy, University of Delaware, Newark, Delaware 19716, United States*

**George W. Luther** − *School of Marine Science and Policy, University of Delaware, Newark, Delaware 19716, United States*

Complete contact information is available at: https://pubs.acs.org/10.1021/acs.est.1c00497


### Notes

The authors declare no competing financial interest.



https://doi.org/10.1021/acs.est.1c00497
Environ. Sci. Technol. 2021, 55, 9362−9371

## ■ ACKNOWLEDGMENTS

This work was funded by NASA Exobiology grant 80NSSC18K1292, NSF EAR grant 1833525 to C.S.C. and the Joanne Daiber Fellowship to N.Z.

## ■ REFERENCES

(1) Borch, T.; Kretzschmar, R.; Kappler, A.; Van Cappellen, P.; Ginder-Vogel, M.; Voegelin, A.; Campbell, K. Biogeochemical Redox Processes and Their Impact on Contaminant Dynamics. *Environ. Sci. Technol.* **2010**, *44*, 15−23.

(2) Ferris, F.; Hallberg, R.; Lyvén, B.; Pedersen, K. Retention of Strontium, Cesium, Lead and Uranium by Bacterial Iron Oxides from a Subterranean Environment. *Appl. Geochemistry* **2000**, *15*, 1035−1042.

(3) Michálková, Z.; Komárek, M.; Šillerová, H.; Della Puppa, L.; Joussein, E.; Bordas, F.; Vaněk, A.; Vaněk, O.; Ettler, V. Evaluating the Potential of Three Fe- and Mn-(Nano)Oxides for the Stabilization of Cd, Cu and Pb in Contaminated Soils. *J. Environ. Manage.* **2014**, *146*, 226−234.

(4) Sodano, M.; Lerda, C.; Nisticò, R.; Martin, M.; Magnacca, G.; Celi, L.; Said-Pullicino, D. Dissolved Organic Carbon Retention by Coprecipitation during the Oxidation of Ferrous Iron. *Geoderma* **2017**, *307*, 19−29.

(5) Zhou, Z.; Latta, D. E.; Noor, N.; Thompson, A.; Borch, T.; Scherer, M. M. Fe(II)-Catalyzed Transformation of Organic Matter-Ferrihydrite Coprecipitates: A Closer Look Using Fe Isotopes. *Environ. Sci. Technol.* **2018**, *52*, 11142−11150.

(6) Pullin, M. J.; Cabaniss, S. E. The Effects of PH, Ionic Strength, and Iron-Fulvic Acid Interactions on the Kinetics of Non-Photochemical Iron Transformations. II. The Kinetics of Thermal Reduction. *Geochim. Cosmochim Acta* **2003**, *67*, 4079−4089.

(7) Pham, A. N.; Waite, T. D. Oxygenation of Fe(II) in the Presence of Citrate in Aqueous Solutions at PH 6.0-8. 0 and 25 °C: Interpretation from an Fe(II)/Citrate Speciation Perspective. *J. Phys Chem. A* **2008**, *112*, 643−651.

(8) Morgan, B.; Lahav, O. The Effect of PH on the Kinetics of Spontaneous Fe(II) Oxidation by O2 in Aqueous Solution-Basic Principles and a Simple Heuristic Description. *Chemosphere* **2007**, *68*, 2080−2084.

(9) Liang, L.; McNabb, J. A.; Paulk, J. M.; Gu, B.; McCarthy, J. F. Kinetics of Fe(II) Oxygenation at Low Partial Pressure of Oxygen in the Presence of Natural Organic Matter. *Environ. Sci. Technol.* **1993**, *27*, 1864−1870.

(10) Adhikari, D.; Zhao, Q.; Das, K.; Mejia, J.; Huang, R.; Wang, X.; Poulson, S. R.; Tang, Y.; Roden, E. E.; Yang, Y. Dynamics of Ferrihydrite-Bound Organic Carbon during Microbial Fe Reduction. *Geochim. Cosmochim. Acta* **2017**, *212*, 221−233.

(11) Fujii, M.; Rose, A. L.; Waite, T. D.; Omura, T. Oxygen and Superoxide-Mediated Redox Kinetics of Iron Complexed by Humic Substances in Coastal Seawater. *Environ. Sci. Technol.* **2010**, *44*, 9337−9342.

(12) Pedersen, H. D.; Postma, D.; Jakobsen, R.; Larsen, O. Fast Transformation of Iron Oxyhydroxides by the Catalytic Action of Aqueous Fe(II). *Geochim. Cosmochim. Acta* **2005**, *69*, 3967−3977.

(13) Emmenegger, L.; Schönenberger, R.; Sigg, L.; Sulzberger, B. Light-Induced Redox Cycling of Iron in Circumneutral Lakes. *Limnol. Oceanogr.* **2001**, *46*, 49−61.

(14) Miller, W. L.; King, D. W.; Lin, J.; Kester, D. R. Photochemical Redox Cycling of Iron in Coastal Seawater. *Mar. Chem.* **1995**, *50*, 63−77.

(15) Jones, A. M.; Griffin, P. J.; Waite, T. D. Ferrous Iron Oxidation by Molecular Oxygen under Acidic Conditions: The Effect of Citrate, EDTA and Fulvic Acid. *Geochim. Cosmochim. Acta* **2015**, *160*, 117−131.

(16) Daugherty, E. E.; Gilbert, B.; Nico, P. S.; Borch, T. Complexation and Redox Buffering of Iron (II) by Dissolved Organic Matter. *Environ. Sci. Technol.* **2017**, *51*, 11096−11104.

(17) Sada, E.; Kumazawa, H.; Machida, H. Oxidation Kinetics of FeII-Edta and FeII-Nta Chelates by Dissolved Oxygen. *Ind. Eng. Chem. Res.* **1987**, *26*, 1468−1472.

(18) Rose, A. L.; Waite, T. D. Kinetics of Iron Complexation by Dissolved Natural Organic Matter in Coastal Waters. *Mar. Chem.* **2003**, *84*, 85−103.

(19) McAllister, S. M.; Moore, R. M.; Gartman, A.; Luther, G. W.; Emerson, D.; Chan, C. S. The Fe(II)-Oxidizing Zetaproteobacteria: Historical, Ecological and Genomic Perspectives. *FEMS Microbiol. Ecol.* **2019**, *95*, 1−18.

(20) Maisch, M.; Lueder, U.; Laufer, K.; Scholze, C.; Kappler, A.; Schmidt, C. Contribution of Microaerophilic Iron (II)-Oxidizers to Iron (III) Mineral Formation. *Environ. Sci. Technol.* **2019**, *53*, 8197−8204.

(21) Druschel, G. K.; Emerson, D.; Sutka, R.; Suchecki, P.; Luther, G. W. Low-Oxygen and Chemical Kinetic Constraints on the Geochemical Niche of Neutrophilic Iron (II) Oxidizing Microorganisms. *Geochim. Cosmochim. Acta* **2008**, *72*, 3358−3370.

(22) Eggerichs, T.; Opel, O.; Otte, T.; Ruck, W. Interdependencies between Biotic and Abiotic Ferrous Iron Oxidation and Influence of PH, Oxygen and Ferric Iron Deposits. *Geomicrobiol. J.* **2014**, *31*, 461−472.

(23) Wu, W.; Swanner, E. D.; Hao, L.; Zeitvogel, F.; Obst, M.; Pan, Y.; Kappler, A. Characterization of the Physiology and Cell-Mineral Interactions of the Marine Anoxygenic Phototrophic Fe(II) Oxidizer Rhodovulum Iodosum-Implications for Precambrian Fe(II) Oxidation. *FEMS Microbiol. Ecol.* **2014**, *88*, 503−515.

(24) Hädrich, A.; Taillefert, M.; Akob, D. M.; Cooper, R. E.; Litzba, U.; Wagner, F. E.; Nietzsche, S.; Ciobota, V.; Rösch, P.; Popp, J.; Küsel, K. Microbial Fe(II) Oxidation by Sideroxydans Lithotrophicus ES-1 in the Presence of Schlöppnerbrunnen Fen-Derived Humic Acids. *FEMS Microbiol. Ecol.* **2019**, *95*, 1−19.

(25) Kügler, S.; Cooper, R. E.; Wegner, C. E.; Mohr, J. F.; Wichard, T.; Küsel, K. Iron-Organic Matter Complexes Accelerate Microbial Iron Cycling in an Iron-Rich Fen. *Sci. Total Environ.* **2019**, *646*, 972−988.

(26) Peng, C.; Bryce, C.; Sundman, A.; Borch, T.; Kappler, A. Organic Matter Complexation Promotes Fe(II) Oxidation by the Photoautotrophic Fe(II)-Oxidizer Rhodopseudomonas Palustris TIE-1. *ACS Earth Sp. Chem.* **2019**, *3*, 531−536.

(27) Rose, A. L.; Waite, T. D. Effect of Dissolved Natural Organic Matter on the Kinetics of Ferrous Iron Oxygenation in Seawater. *Environ. Sci. Technol.* **2003**, *37*, 4877−4886.

(28) Krishnamurti, G. S. R. Influence of Citrate on the Kinetics of Fe(II) Oxidation and the Formation of Iron Oxyhydroxides 1. *Clays Clay Miner.* **1991**, *39*, 28−34.

(29) Rose, A. L.; Waite, T. D. Kinetic Model for Fe(II) Oxidation in Seawater in the Absence and Presence of Natural Organic Matter. *Environ. Sci. Technol.* **2002**, *36*, 433−444.

(30) Miller, C. J.; Rose, A. L.; Waite, T. D. Impact of Natural Organic Matter on H2O2-Mediated Oxidation of Fe(II) in a Simulated Freshwater System. *Geochim. Cosmochim. Acta* **2009**, *73*, 2758−2768.

(31) Kügler, S.; Cooper, R. E.; Wegner, C. E.; Mohr, J. F.; Wichard, T.; Küsel, K. Iron-Organic Matter Complexes Accelerate Microbial Iron Cycling in an Iron-Rich Fen. *Sci. Total Environ.* **2019**, *646*, 972−988.

(32) Kopf, S. H.; Henny, C.; Newman, D. K. Ligand-Enhanced Abiotic Iron Oxidation and the Effects of Chemical versus Biological Iron Cycling in Anoxic Environments. *Environ. Sci. Technol.* **2013**, *47*, 2602−2611.

(33) McAllister, S. M.; Polson, S. W.; Butterfield, D. A.; Glazer, B. T.; Sylvan, J. B.; Chan, C. S. Validating the Cyc 2 Neutrophilic Iron Oxidation Pathway Using Meta-Omics of Zetaproteobacteria</Em> Iron Mats at Marine Hydrothermal Vents. *mSystems* **2020**, *5*, No. e00553.

(34) Emerson, D.; Moyer, C. Isolation and Characterization of Novel Iron-Oxidizing Bacteria That Grow at Circumneutral PH. *Appl. Environ. Microbiol.* **1997**, *63*, 4784−4792.



https://doi.org/10.1021/acs.est.1c00497
*Environ. Sci. Technol.* 2021, 55, 9362−9371

(35) Smith, R. M.; Martell, A. E. *NIST Critically Selected Stability Constant of Metal Complexes Database*; *Version 4* National Institute of Standards and Technology: Gaithersburg, MD, 1997.
(36) Doud, D. F. R.; Angenent, L. T. Toward Electrosynthesis with Uncoupled Extracellular Electron Uptake and Metabolic Growth: Enhancing Current Uptake with Rhodopseudomonas Palustris. *Environ. Sci. Technol. Lett.* **2014**, *1*, 351−355.
(37) Picardal, F. W.; Zaybak, Z.; Chakraborty, A.; Schieber, J.; Szewzyk, U. Microaerophilic, Fe(II)-Dependent Growth and Fe(II) Oxidation by a Dechlorospirillum Species. *FEMS Microbiol. Lett.* **2011**, *319*, 51−57.
(38) Kadier, A.; Abdeshahian, P.; Kalil, M. S.; Hasan, H. A.; Hamid, A. A. Optimization of the Key Medium Components and Culture Conditions for Efficient Cultivation of G. Sulfurreducens Strain PCA ATCC 51573 Using Response Surface Methodology. *Iran. J. Sci. Technol. Trans A Sci.* **2018**, *42*, 237−244.
(39) Amonette, J. E.; Templeton, J. C. Improvements to the Quantitative Assay of Nonrefractory Minerals for Fe(II) and Total Fe Using 1, 10-Phenanthroline. *Clays Clay Miner.* **1998**, *46*, 51−62.
(40) Gustafsson, J. P. Visual MINTEQ 3.0 User Guide. *Dep. of L. Water Resour.Eng.* **2012**, 1−73.
(41) Kinniburgh, D. G.; Milne, C. J.; Benedetti, M. F.; Pinheiro, J. P.; Filius, J.; Koopal, L. K.; Van Riemsdijk, W. H. Metal Ion Binding by Humic Acid: Application of the NICA-Donnan Model. *Environ. Sci. Technol.* **1996**, *30*, 1687−1698.
(42) Vidali, R.; Remoundaki, E.; Tsezos, M. An Experimental and Modeling Study of Humic Acid Concentration Effect on H+ Binding: Application of the NICA−Donnan Model. *J. Colloid Interface Sci.* **2009**, *339*, 330−335.
(43) Yan, M.; Benedetti, M. F.; Korshin, G. V. Study of Iron and Aluminum Binding to Suwannee River Fulvic Acid Using Absorbance and Fluorescence Spectroscopy: Comparison of Data Interpretation Based on NICA-Donnan and Stockholm Humic Models. *Water Res.* **2013**, *47*, 5439−5446.
(44) Stumm, W.; Lee, G. F. Oxygenation of Ferrous Iron. *Ind. Eng. Chem.* **1961**, *53*, 143−146.
(45) Millero, F. J.; Sotolongo, S.; Izaguirre, M. The Oxidation Kinetics of Fe(II) in Seawater. *Geochim. Cosmochim. Acta* **1987**, *51*, 793−801.
(46) Mullaugh, K. M.; Luther, G. W.; Ma, S.; Moore, T. S.; Yücel, M.; Becker, E. L.; Podowski, E. L.; Fisher, C. R.; Trouwborst, R. E.; Pierson, B. K. Voltammetric (Micro) Electrodes for the in Situ Study of Fe2+ Oxidation Kinetics in Hot Springs and S2O32- Production at Hydrothermal Vents. *Electroanalysis* **2008**, *20*, 280−290.
(47) Zhang, Y.; Zhou, M. A Critical Review of the Application of Chelating Agents to Enable Fenton and Fenton-like Reactions at High PH Values. *J. Hazard. Mater.* **2019**, *362*, 436−450.
(48) Krom, B. P.; Warner, J. B.; Konings, W. N.; Lolkema, J. S. Complementary Metal Ion Specificity of the Metal-Citrate Transporters Cit M and Cit H of Bacillus Subtilis. *J. Bacteriol.* **2000**, *182*, 6374−6381.
(49) Grzybowski, A. K.; Datta, S. P. The Stability Constants of Magnesium Citrate Complexes. *J. Chem. Soc.* **1964**, 3905−3912.
(50) Luther, G. W.; Kostka, J. E.; Church, T. M.; Sulzberger, B.; Stumm, W. Seasonal Iron Cycling in the Salt-Marsh Sedimentary Environment: The Importance of Ligand Complexes with Fe(II) and Fe(III) in the Dissolution of Fe(III) Minerals and Pyrite, Respectively. *Mar. Chem.* **1992**, *40*, 81−103.
(51) Lee, S.; Roh, Y.; Koh, D.-C. Oxidation and Reduction of Redox-Sensitive Elements in the Presence of Humic Substances in Subsurface Environments: A Review. *Chemosphere* **2019**, *220*, 86−97.
(52) Krachler, R.; Krachler, R. F.; Wallner, G.; Hann, S.; Laux, M.; Cervantes Recalde, M. F.; Jirsa, F.; Neubauer, E.; von der Kammer, F.; Hofmann, T.; Keppler, B. K. River-Derived Humic Substances as Iron Chelators in Seawater. *Mar. Chem.* **2015**, *174*, 85−93.
(53) Stern, N.; Mejia, J.; He, S.; Yang, Y.; Ginder-Vogel, M.; Roden, E. E. Dual Role of Humic Substances As Electron Donor and Shuttle for Dissimilatory Iron Reduction. *Environ. Sci. Technol.* **2018**, *52*, 5691−5699.
(54) Aeschbacher, M.; Sander, M.; Schwarzenbach, R. P. Novel Electrochemical Approach to Assess the Redox Properties of Humic Substances. *Environ. Sci. Technol.* **2010**, *44*, 87−93.
(55) Aeschbacher, M.; Vergari, D.; Schwarzenbach, R. P.; Sander, M. Electrochemical Analysis of Proton and Electron Transfer Equilibria of the Reducible Moieties in Humic Acids. *Environ. Sci. Technol.* **2011**, *45*, 8385−8394.
(56) Klüpfel, L.; Piepenbrock, A.; Kappler, A.; Sander, M. Humic Substances as Fully Regenerable Electron Acceptors in Recurrently Anoxic Environments. *Nat. Geosci.* **2014**, *7*, 195−200.
(57) Bauer, M.; Blodau, C. Arsenic Distribution in the Dissolved, Colloidal and Particulate Size Fraction of Experimental Solutions Rich in Dissolved Organic Matter and Ferric Iron. *Geochim. Cosmochim. Acta* **2009**, *73*, 529−542.
(58) Aeschbacher, M.; Graf, C.; Schwarzenbach, R. P.; Sander, M. Antioxidant Properties of Humic Substances. *Environ. Sci. Technol.* **2012**, *46*, 4916−4925.
(59) Liu, Y.; Zheng, X.; Yin, S.; Wei, C.; Zhu, D. A Significant Correlation between Kinetics of Nitrobenzene Reduction by Sulfide and Electron Transfer Capacity of Mediating Dissolved Humic Substances. *Sci. Total Environ.* **2020**, *740*, No. 139911.
(60) Jones, A. M.; Griffin, P. J.; Collins, R. N.; Waite, T. D. Ferrous Iron Oxidation under Acidic Conditions−The Effect of Ferric Oxide Surfaces. *Geochim. Cosmochim. Acta* **2014**, *145*, 1−12.
(61) Jeon, B.-H.; Dempsey, B. A.; Burgos, W. D. Kinetics and Mechanisms for Reactions of Fe(II) with Iron (III) Oxides. *Environ. Sci. Technol.* **2003**, *37*, 3309−3315.
(62) Park, B.; Dempsey, B. A. Heterogeneous Oxidation of Fe(II) on Ferric Oxide at Neutral PH and a Low Partial Pressure of O 2 †. *Environ. Sci. Technol.* **2005**, *39*, 6494−6500.
(63) Vantelon, D.; Davranche, M.; Marsac, R.; La Fontaine, C.; Guénet, H.; Jestin, J.; Campaore, G.; Beauvois, A.; Briois, V. Iron Speciation in Iron-Organic Matter Nanoaggregates: A Kinetic Approach Coupling Quick-EXAFS and MCR-ALS Chemometrics. *Environ. Sci. Nano* **2019**, *6*, 2641−2651.
(64) Angelico, R.; Ceglie, A.; He, J.-Z.; Liu, Y.-R.; Palumbo, G.; Colombo, C. Particle Size, Charge and Colloidal Stability of Humic Acids Coprecipitated with Ferrihydrite. *Chemosphere* **2014**, *99*, 239−247.
(65) Liao, P.; Li, W.; Jiang, Y.; Wu, J.; Yuan, S.; Fortner, J. D.; Giammar, D. E. Formation, Aggregation, and Deposition Dynamics of Nom-Iron Colloids at Anoxic-Oxic Interfaces. *Environ. Sci. Technol.* **2017**, *51*, 12235−12245.
(66) Pédrot, M.; Le Boudec, A.; Davranche, M.; Dia, A.; Henin, O. How Does Organic Matter Constrain the Nature, Size and Availability of Fe Nanoparticles for Biological Reduction? *J. Colloid Interface Sci.* **2011**, *359*, 75−85.
(67) Garg, S.; Jiang, C.; David Waite, T. Mechanistic Insights into Iron Redox Transformations in the Presence of Natural Organic Matter: Impact of PH and Light. *Geochim. Cosmochim. Acta* **2015**, *165*, 14−34.
(68) Pullin, M. J.; Cabaniss, S. E. The Effects of PH, Ionic Strength, and Iron-Fulvic Acid Interactions on the Kinetics of Non-Photochemical Iron Transformations. I. Iron (II) Oxidation and Iron (III) Colloid Formation. *Geochim. Cosmochim. Acta* **2003**, *67*, 4067−4077.
(69) Garg, S.; Jiang, C.; Waite, T. D. Impact of PH on Iron Redox Transformations in Simulated Freshwaters Containing Natural Organic Matter. *Environ. Sci. Technol.* **2018**, *52*, 13184−13194.
(70) Voelker, B. M.; Sulzberger, B. Effects of Fulvic Acid on Fe(II) Oxidation by Hydrogen Peroxide. *Environ. Sci. Technol.* **1996**, *30*, 1106−1114.
(71) Pham, A. N.; Rose, A. L.; Waite, T. D. Kinetics of Cu(II) Reduction by Natural Organic Matter. *J. Phys. Chem. A* **2012**, *116*, 6590−6599.
(72) Chen, C.; Thompson, A. Ferrous Iron Oxidation under Varying PO2 Levels: The Effect of Fe(III)/Al (III) Oxide Minerals and Organic Matter. *Environ. Sci. Technol.* **2018**, *52*, 597−606.
(73) Peng, C.; Bryce, C.; Sundman, A.; Kappler, A. Cryptic Cycling of Complexes Containing Fe(III) and Organic Matter by Photo-


https://doi.org/10.1021/acs.est.1c00497
*Environ. Sci. Technol.* 2021, 55, 9362−9371

trophic Fe(II)-Oxidizing Bacteria. *Appl. Environ. Microbiol.* **2019**, *85* (), DOI: 10.1128/AEM.02826-18.
(74) Schmid, G.; Zeitvogel, F.; Hao, L.; Ingino, P.; Floetenmeyer, M.; Stierhof, Y.-D.; Schroeppel, B.; Burkhardt, C. J.; Kappler, A.; Obst, M. 3-D Analysis of Bacterial Cell-(Iron) Mineral Aggregates Formed during Fe(II) Oxidation by the Nitrate-Reducing Acidovorax Sp. Strain BoFeN1 Using Complementary Microscopy Tomography Approaches. *Geobiology* **2014**, *12*, 340−361.
(75) Miot, J.; Benzerara, K.; Morin, G.; Kappler, A.; Bernard, S.; Obst, M.; Férard, C.; Skouri-Panet, F.; Guigner, J.-M.; Posth, N.; Guyot, F. Iron Biomineralization by Anaerobic Neutrophilic Iron-Oxidizing Bacteria. *Geochim. Cosmochim. Acta* **2009**, *73*, 696−711.
(76) Peng, C.; Sundman, A.; Bryce, C.; Catrouillet, C.; Borch, T.; Kappler, A. Oxidation of Fe(II)-Organic Matter Complexes in the Presence of the Mixotrophic Nitrate-Reducing Fe(II)-Oxidizing Bacterium Acidovorax Sp. BoFeN1. *Environ. Sci. Technol.* **2018**, *52*, 5753−5763.
(77) Cooper, R. E.; Wegner, C.-E.; McAllister, S. M.; Shevchenko, O.; Chan, C. S.; Küsel, K. Draft Genome Sequence of Sideroxydans Sp. Strain CL21, an Fe (II)-Oxidizing Bacterium. *Microbiol. Resour. Announc.* **2020**, *9* (), DOI: 10.1128/MRA.01444-19.
(78) Lüdecke, C.; Reiche, M.; Eusterhues, K.; Nietzsche, S.; Küsel, K. Acid-Tolerant Microaerophilic Fe(II)-Oxidizing Bacteria Promote Fe(III)-Accumulation in a Fen. *Environ. Microbiol.* **2010**, *12*, 2814−2825.
(79) Cao, D.; Hao, Z.; Hu, M.; Geng, F.; Rao, Z.; Niu, H.; Shi, Y.; Cai, Y.; Zhou, Y.; Liu, J.; Kang, Y. A Feasible Strategy to Improve Confident Elemental Composition Determination of Compounds in Complex Organic Mixture Such as Natural Organic Matter by FTICR-MS without Internal Calibration. *Sci. Total Environ.* **2021**, *751*, No. 142255.
(80) Derenne, S.; Nguyen Tu, T. T. Characterizing the Molecular Structure of Organic Matter from Natural Environments: An Analytical Challenge. *Comptes Rendus Geosci.* **2014**, *346*, 53−63.
(81) Amstaetter, K.; Borch, T.; Kappler, A. Influence of Humic Acid Imposed Changes of Ferrihydrite Aggregation on Microbial Fe(III) Reduction. *Geochim. Cosmochim. Acta* **2012**, *85*, 326−341.
(82) Lovley, D. R.; Blunt-Harris, E. L. Role of Humic-Bound Iron as an Electron Transfer Agent in Dissimilatory Fe(III) Reduction. *Appl. Environ. Microbiol.* **1999**, *65*, 4252−4254.
(83) Wolf, M.; Kappler, A.; Jiang, J.; Meckenstock, R. U. Effects of Humic Substances and Quinones at Low Concentrations on Ferrihydrite Reduction by Geobacter Metallireducens. *Environ. Sci. Technol.* **2009**, *43*, 5679−5685.


https://doi.org/10.1021/acs.est.1c00497
*Environ. Sci. Technol.* 2021, 55, 9362−9371